JOURNAL OF COMPUTATIONAL PHYSICS 58, 134–145 (1985)

Acoustic Shocks in a Variable Area Duct Containing Near Sonic Flows

S. I. HARIHARAN*

University of Tennessee Space Institute, Tullahoma, Tennessee 37388 and Institute for Computer Applications in Science and Engineering

AND

HAROLD C. LESTER

NASA Langley Research Center, Hampton, Virginia 23665

Received November 29, 1983; revised May 23, 1984

In this paper acoustic shock waves are considered in a variable area duct which contains near sonic flows. The problem treated here is modelled after an aero engine inlet. It is known experimentally that area variation of a duct and high Mach number mean flow can reduce acoustical energy yielding substantial noise reduction. One possible reason for this is acoustic shocks. The use of an explicit numerical method is described which is very accurate and also captures shocks reasonably well. Comparisons of the results are made with an existing asymptotic theory for Mach numbers close to unity. When shock occurs reduction of sound pressure levels are shown by examples.

1. INTRODUCTION

Recently a numerical solution for the propagation of sound in a variable area duct which contains a high Mach number subsonic flow was studied by the authors [4]. The nature of the wave propagation was nonlinear. This note is a continuation of this work and presents some results concerning computations of shocked waves in this situation. The model problem studied here and in [4] serves the purpose of the study of an aero engine inlet. Briefly there is a flow in a variable area duct and acoustic waves propagate upstream of this flow. The acoustic waves are generated by an incident plane wave on the left of the duct and leave the right end without reflecting. It was first observed experimentally [3] that with a given flow and a proper choice of area variation it is possible to attenuate the sound intensity as much as 20db. Theoretical reasons for this mechanism of reduction of noise level

* Research for this author was supported by the National Aeronautics and Space Administration under NASA Contracts NAS1-17070 and NAS1-17130 while he was in residence at ICASE, NASA Langley Research Center, Hampton, VA 23665.

0021-9991/85 $3.00

are still under investigation. They are complicated by the fluid equations which are the Navier–Stokes equations. However, in the inviscid limit it is believed [7, 8] that acoustic shocks which result in energy loss is one such possibility. Though sound level attenuation was not shown in [7], they did show energy loss when shocks occur. The work in [7] is based on an asymptotic theory and valid for Mach numbers close to unity. In a later experimental study [5] it was shown that even for Mach numbers far less than unity (about 0.7) one still obtains substantial sound reduction. Thus a numerical study was undertaken to calculate solutions for all Mach numbers.

There has been only a little published in the literature for this flow configuration. The classical Fubini solution uses an asymptotic expansion to obtain an approximate solution to the one-dimensional gas dynamic equation for a uniform duct. Polyakova [10] made extensions for problems with flow and Blackstock [1] for the case of shocks. For variable area ducts Myers and Calleghari [8] used the method of matched asymptotic expansions. This reference was the only source for any constructive shock solution in the literature. Recently parallel to our work Walkington and Eversman [12] carried out computations of this situation. Our study yields similar results but we believe our approach is simpler for the reasons that we solve a system of two equations using isentropic relations instead of a system of three equations. This is discussed in the next section. Moreover, the scheme used here has more spatial accuracy than the one in [12]. This is particularly true when we seek smooth solutions, since we do not add any artificial damping for these situations. The authors would like to point out that there has been other work namely Nayfeh *et al.* [9] to compute the nonlinear, but unshocked solutions for this type of configuration.

In this work we describe the model briefly and indicate the assembly of the numerical method. We emphasize the approach we took for obtaining boundary conditions. We present numerical results obtained for shock cases and compare with the asymptotic results of [7]. We also present noise level distribution over the duct and demonstrate the noise reduction in the situation of a shock.

The authors would like to acknowledge useful comments and suggestions of referees.

2. Equations of motion

The total flow field is governed by the inviscid, compressible Euler equations. They consist of equations for continuity, momentum, and energy. The energy equation can be replaced by isentropic relations provided one is seeking only weak shocks. This is exactly the case in acoustics where only weak shocks are the central goal. Strong shocks causes disturbances in the main stream and the meaning of acoustics will not be valid. This philosophy was adapted in [4] and it yielded a system of two equations for acoustic density and velocity rather than three equations thus reducing computational costs.

The situation which is of interest here assumes a quasi one dimensional flow. Flow configuration is depicted in Fig. 1. In this a steady flow moving from the left to right and the acoustic waves are propagating upstream of the flow from a harmonically varying source (plane wave). Then the total field is governed by the following equations, where $A(x)$ is the area variation of the duct

$$\frac{\partial \bar{\rho}}{\partial t} + \frac{\partial}{\partial x}(\bar{\rho}\bar{u}) + \frac{\bar{\rho}\bar{u}}{A}\frac{dA}{dx} = 0 \tag{2.1}$$

$$\frac{\partial \bar{u}}{\partial t} + \frac{\partial}{\partial x}\left(\frac{\bar{u}^2}{2} + \frac{\gamma}{\gamma - 1}\frac{p_0}{\rho_0^\gamma}\bar{\rho}^{\gamma-1}\right) = 0 \tag{2.2}$$

and the pressure is determined from

$$\bar{p} = \frac{p_0}{\rho_0^\gamma}\bar{\rho}^\gamma. \tag{2.3}$$

Here $\bar{\rho}$, $\bar{u}$, and $\bar{p}$ are the total density, velocity, and pressure, respectively, and the quantities with subscript zero denote ambient values. We divide these flow quantities into "mean" and "acoustic" parts. That is, if mean flow quantities are assigned a subscript s then

$$\begin{aligned} \bar{u} &= u_s + u \\ \bar{\rho} &= \rho_s + \rho \\ \bar{p} &= p_s + p. \end{aligned} \tag{2.4}$$

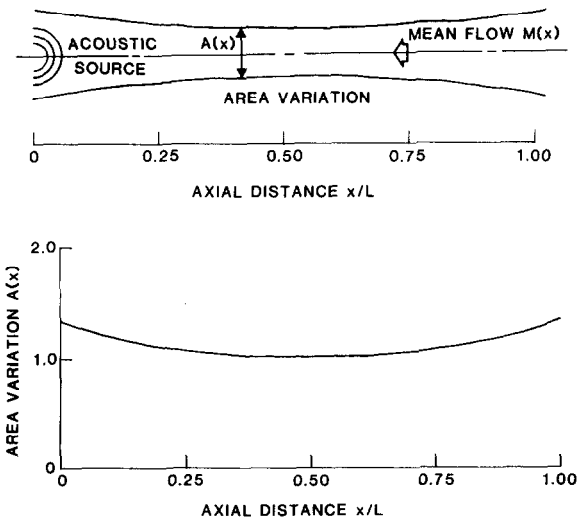

FIG. 1. Variable area flow duct (a) coordinate geometry, and (b) area variation.

The mean flow is assumed to be steady and they satisfy the following steady state flow equations:

$$\frac{\partial}{\partial x}(u_s\rho_s)+\frac{\rho_s u_s}{A}\frac{dA}{dx}=0 \tag{2.5}$$

$$\frac{\partial}{\partial x}\left(\frac{U_s^2}{2}+\frac{\gamma}{\gamma-1}\frac{p_0}{\rho_0^\gamma}\rho_s^{\gamma-1}\right)=0 \tag{2.6}$$

$$p_s=\frac{p_0}{\rho_0^\gamma}\rho_s^\gamma. \tag{2.7}$$

Then Eqs. (2.1)–(2.3) yield the following nondimensional acoustic equations,

$$\rho_t+(u_s\rho+\rho_s u+u\rho)_x+(u_s\rho+\rho_s u+u\rho)\frac{1}{A}\frac{dA}{dx}=0 \tag{2.8}$$

$$u_t+\left[u_s u+\frac{u^2}{2}+c_s^2\left(\rho/\rho_s+\frac{\gamma-2}{2}(\rho/\rho_s)^2\right)\right]_x=0 \tag{2.9}$$

$$p=c_s^2\left(1+\frac{\gamma-1}{2}\rho/\rho_s\right)\rho. \tag{2.10}$$

Here c_s is the local sound speed in the flow and is given by

$$c_s^2=\gamma\frac{p_s}{\rho_s}. \tag{2.11}$$

The details of derivation of these equations are available in [4]. Note that in these equations density and velocity are scaled by their ambient values ρ_0 and C_0, the pressure is scaled by $\rho_0 C_0^2$, and the area by the throat area A_t of the duct. Moreover the distance and time are scaled by w/C_0 and by w, where w is the frequency of the source. This frequency corresponds to the engine noise source. In this nondimensionalization process the meanflow becomes the Mach number distribution and the solution space becomes the interval $[0, L]$, where L is the duct length multiplied by w/C_0. These equations are to be solved subject to the following boundary conditions. At $x=0$,

$$u(0, t)=f(t) \qquad (t>0), \tag{2.12}$$

At $x=L$,

$$B(u, \rho)(L, t)=0, \tag{2.13}$$

where $f(t)$ is the source variation and (2.13) dictates a nonreflective (impedance type) condition. We shall derive this condition in Section 4.

3. Numerical Scheme

We shall briefly indicate the numerical method used in this work. This method is simply an extended version of MacCormack's method with fourth-order accuracy in space and second-order accuracy in time (see [2]). One can minimize the truncation error in time by choosing sufficiently small time steps (or lower CFL values) to get the fourth-order accuracy in space. Let the spatial discretization of the axis of the duct be given by $x_j = (j-1)\,L/J$ $(j = 1,..., J)$. Let us define forward and backward flux difference operators by

$$P_J^{\pm}(f) = 7f_j - 8f_{j\pm 1} + f_{j\pm 2}. \tag{3.1}$$

Here the plus "sign" denotes forward and "minus" sign denotes backward operations, respectively. Then for a single equation of the form

$$u_t + f_x = h, \tag{3.2}$$

the scheme works as follows:

$$\begin{aligned} u_j^{(1)} &= u_j^n - \frac{\Delta t/2}{6\Delta x} P_j^-(f^n) + \frac{\Delta t}{2} h_j^n \\ u_j^{n+1/2} &= \frac{1}{2}\left[u_j^n + u_j^{(1)} + \frac{\Delta t/2}{6\Delta x} P_j^+(f^{(1)}) + \frac{\Delta t}{2} h_j^{(1)} \right]. \end{aligned} \tag{3.3}$$

This has a backward predictor and a forward corrector. In the next $\Delta t/2$ time step it is changed into a forward predictor and a backward corrector as follows:

$$\begin{aligned} u_j^{(1)} &= u_j^{n+1/2} + \frac{\Delta t/2}{6\Delta x} P_j^+(f^{n+1/2}) + \frac{\Delta t}{2} h^{n+1/2} \\ u_j^{n+1} &= \frac{1}{2}\left[u_j^{n+1/2} + u_j^{(1)} - \frac{\Delta t/2}{6\Delta x} P_j^-(f^{(1)}) + \frac{\Delta t}{2} h^{(1)} \right]. \end{aligned} \tag{3.4}$$

In these formulas superscripts n, $n+\frac{1}{2}$ and $n+1$ denote quantities evaluated at times $n\,\Delta t$, $(n+\frac{1}{2})\,\Delta t$ and $(n+1)\,\Delta t$ and the superscript (1) denotes the predicted values. It is pointed out in [9] that alternating formulas (3.3) and (3.4) at each time step is necessary to achieve fourth-order accuracy for nonlinear problems.

We note in (3.3) and (3.4) the flux difference operator P^+ is not defined for $j = J-1$ and $j = J$ and P^- is not defined for $j = 1$ and $j = 0$. At these points fluxes are extrapoled according to the following third-order formula:

$$f_j = 4f_{j+1} - 6f_{j+2} + 4f_{j+3} - f_{j+4} \qquad (j = 0, -1) \tag{3.5}$$

$$f_{j+1} = 4f_j - 6f_{j-1} + 4f_{j-2} - f_{j-3} \qquad (j = J, J+1). \tag{3.6}$$

When these extrapolations are applied to define the fluxes then the steps (3.3) and (3.4) are valid for all grid points $j=1$ through J.

This process is then applied to Eq. (2.8) with

$$u=\rho$$

$$f=u_s\rho+\rho_s u+u\rho$$

and

$$h=-(u_s\rho+\rho_s u+u\rho)\frac{1}{A}\frac{dA}{dx}$$

and to (2.9) with

$$u=u$$

$$f=u_s u+\frac{u^2}{2}+c_s^2\left(\rho/\rho s+\frac{\gamma-2}{2}(\rho/\rho_s)^2\right)$$

and $h=0$.

Artificial Viscosity

Similar to fluid dynamic calculations, in order to capture shock waves without oscillations, viscous damping terms are added to the difference equations. The numerical scheme above is a dissipative scheme and therefore we will show results with and without artificial viscosity. A second-order viscous term is used herein. If the Eqs. (2.8) and (2.9) are written in the form

$$\mathbf{w}_t+\mathbf{f}(\mathbf{w})_x=H(\mathbf{w})$$

where (3.7)

$$\mathbf{w}=\begin{pmatrix}\rho\\ u\end{pmatrix},$$

then the artificial viscous term added to (3.7) is

$$\nu\frac{\partial}{\partial x}\left(|\rho_x|\frac{\partial \mathbf{w}}{\partial x}\right), \tag{3.8}$$

where $\nu=O(1)$. We differenced this quantity according to the following formula:

$$(\Delta x)^2\,\nu\frac{\partial}{\partial x}\left(|\rho_x|\frac{\partial \mathbf{w}}{\partial x}\right)\approx\frac{\nu}{\Delta x}\left[|\rho_{j+1}-\rho_j|\,(\mathbf{w}_{j+1}-\mathbf{w}_j)\right.$$
$$\left.-|\rho_j-\rho_{j-1}|\,(\mathbf{w}_j-\mathbf{w}_{j-1})\right]. \tag{3.9}$$

This is a second-order formula. This formula to be used in both stages of our scheme up to the boundary. The added viscosity terms tend to reduce the accuracy of the scheme. Nevertheless it provided better results than other types of viscosity models, i.e., gave a sharper shock with reasonably accurate solutions in the smooth regions. We shall see this later in our comparison with the asymptotic method of [7].

4. Boundary Conditions

In this section we consider some questions concerning boundary conditions. First we need a nonreflective boundary condition at the exit section of the duct. Next we need boundary conditions appropriate to the numerical scheme. These are accomplished by obtaining characteristic variables for the system (2.4) and (2.5). We linearize this system to get

$$\mathbf{w}_t + A\mathbf{w}_x = 0, \tag{4.1}$$

where

$$A = \begin{pmatrix} u_s & \rho_s \\ \dfrac{c_s^2}{\rho_s} & u_s \end{pmatrix} \quad \text{and} \quad \mathbf{w} = \begin{pmatrix} \rho \\ u \end{pmatrix}.$$

The eigenvalues of this matrix are

$$\lambda_+ = u_s + c_s \quad \text{and} \quad \lambda_- = u_s - c_s.$$

We note that $u_s < c_s$ thus λ_- is strictly negative. The signs of these eigenvalues give the characteristic directions of the flow. At $x = 0$, $\lambda_+ > 0$ gives the inflow direction and $\lambda_- < 0$ gives the outflow direction. Similarly at $x = L$, $\lambda_+ > 0$ gives the outflow and λ_- inflow directions, respectively. The matrix formed by the eigenvectors is

$$T = \begin{pmatrix} 1 & 1 \\ \dfrac{c_s}{\rho_s} & \dfrac{-c_s}{\rho_s} \end{pmatrix} \tag{4.2}$$

so that $T^{-1}AT$ is diagonal. The characteristic variables are then

$$\mathbf{v} = T^{-1}\mathbf{w}. \tag{4.3}$$

If

$$\mathbf{v} = \begin{pmatrix} v_1 \\ v_2 \end{pmatrix}$$

then

$$v_1 = \frac{\rho}{\rho_s} + \frac{u}{c_s}$$
$$v_2 = \frac{\rho}{\rho_s} - \frac{u}{c_s}. \tag{4.4}$$

Here v_1, v_2 corresponds to the eigenvalues λ_+ and λ_-, respectively. At $x = L$, v_2 is the inflow variable. Setting $v_2 = 0$, i.e.,

$$\frac{\rho}{\rho_s} - \frac{u}{c_s} = 0 \tag{4.5}$$

is exactly the nonreflective condition stated by the general form in (2.13). In linear acoustics this is known as the impedence condition.

For the numerical scheme it was found effective prescribing the boundary conditions in terms of these variables v_1 and v_2. At $x = 0$, v_2 is computed through an iteration. Let us call this value v_2^c. Thus

$$\frac{\rho}{\rho_s} - \frac{u}{c_s} = v_2^c. \tag{4.6}$$

But u is prescribed at $x = 0$,

$$u = f. \tag{4.7}$$

Solving (4.7) and (4.6) for u and ρ we have

$$u = f; \qquad \rho = \rho_s \left(v_2^c + \frac{f}{c_s} \right). \tag{4.8}$$

Similarly at $x = L$ we compute v_1; this gives

$$\frac{\rho}{\rho_s} + \frac{u}{c_s} = v_1^c. \tag{4.10}$$

We solve (4.5) and (4.10) to obtain the values of u and ρ at $x = L$. They are

$$\rho = \rho_s v_1^c/2$$
$$u = c_s v_1^c/2. \tag{4.11}$$

Together with these conditions the solutions were started at a state of rest and iterated over 6 periods to obtain the results discussed in the next section.

5. Discussion of Results

The procedures developed in the previous sections were applied to a particular geometry called a Crocco–Tsien duct. A detailed description of the contour of the duct is available in [6]. This contour is designed in such a way that the mean flow accelerates linearly to Mach number unity at the throat. In particular, for the examples given here the entry Mach number at the exit section was -0.50 and at the throat -0.90 $(=M_t)$. Here the "minus" sign denotes the flow in the negative x direction.

Figure 1a shows a typical configuration of the duct. Figure 1b shows the area variation. This geometry has an exit/throat ratio about 1.32, so that this area variation provides a gradual choking of the flow. In this case the Mach number distribution becomes as depicted in Fig. 2. With this area variation and Mach number distribution, the steady flow equations satisfied by ρ_s and u_s (Eqs. (2.5) and (2.6)) were solved explicitly (see also [4]).

As we discussed previously, the finite difference algorithm is compared with the asymptotic theory developed in [7]. Since the typical nonlinear situation arises at higher sound pressure levels and Mach numbers approaching unity, in this theory a small perturbation parameter was chosen as $(1-|M_t|)$, where M_t is the throat Mach number. Comparisons for a value for $M_t = -0.90$ are given in Figs. 3 and 5, respectively. The strengths for an equivalent sound pressure source located at $x=0$ (Fig. 1a) are roughly 149 and 156dB, respectively. Corresponding to Eq. (2.12) they have the form

$$f(t) = A \cos t,$$

where A is the amplitude calculated according to the source strength. In both (149dB and 156dB) cases shocks wre predicted in [7]. In these figures the time history of the velocity over a period (2π) is given. The velocity is normalized by $(1-|M_t|)^2$ since the acoustic velocity is small in magnitude. Thus the actual value of the acoustic velocity is of the order 10^{-3} or less away from shocks. Thus an accurate scheme is always preferred for these calculations. However, in the cases of

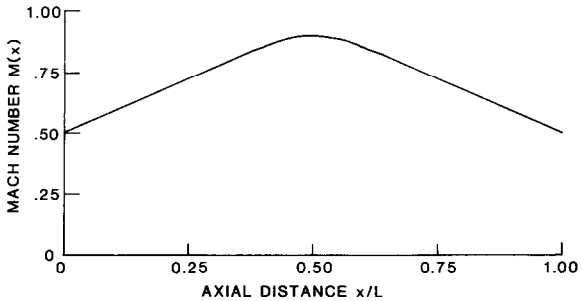

Fig. 2. Mean flow Mach number $M_t = 0.90$.

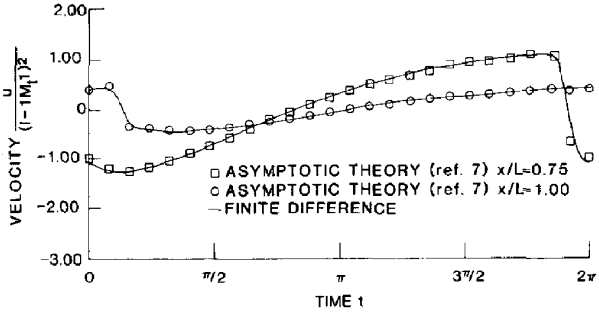

FIG. 3. Acoustic particle velocity, 149dB source, $M_t = -0.90$.

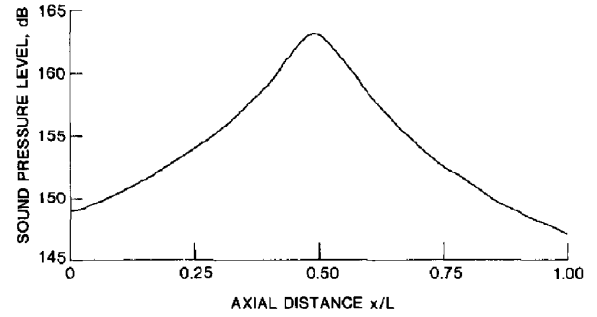

FIG. 4. Acoustic pressure, 149dB source, $M_t = -0.90$.

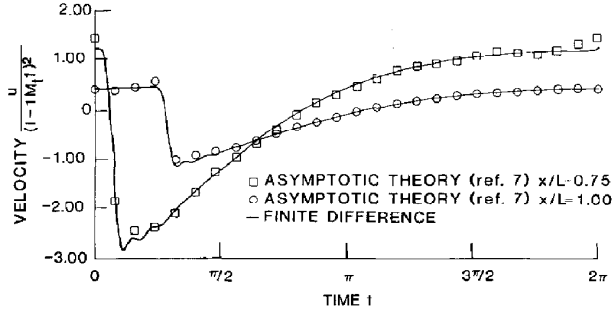

FIG. 5. Acoustic particle velocity, 156dB source, $M_t = -0.90$.

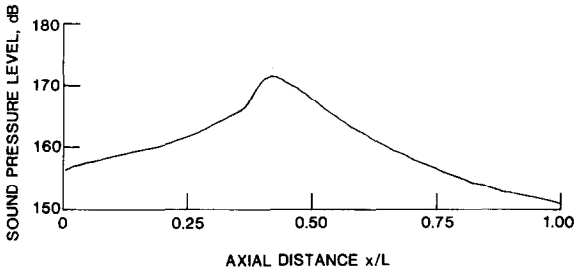

FIG. 6. Acoustic pressure, 156dB source, $M_t = -0.90$.

shock waves, we settle for a little less accuracy to improve the shock structure (i.e., second-order). Thus the purpose of using a fourth-order scheme is to improve the accuracy of smooth solutions in which case the artificial viscosity will not be used. The solid lines in these figures are the numerical solutions and the other (see Figs. 3 and 5) are the asymptotic solutions computed at $x = 0.75L$ and at the exist $x = L$, respectively. The difference scheme we used itself is a dissipative scheme. We carried out the computations without artificial viscosity terms in the algorithm. For the case of 149dB source the results are shown in Fig. 7. The comparison is still good in the smooth regions. Results shown in Figs. 3 and 7 also validate the fact that the amount of added artificial viscosity did not affect the physics of the wave nature.

Finally, Figs. 4 and 6 show the overall sound pressure level (dB) in the duct. Figure 4 corresponds to the shock case of 149dB sound source. This is a very weak shock case. At the exit we see a 2dB sound pressure level reduction. Figure 6 shows the sound pressure level for a 156dB source. In this case we see a sound pressure level reduction about 5dB at the exit. These results show that the higher the sound source level one obtains substantial sound reduction through loss of energy due to shocks.

Extension of this work in two dimensions is in progress by the authors. The results will be reported elsewhere.

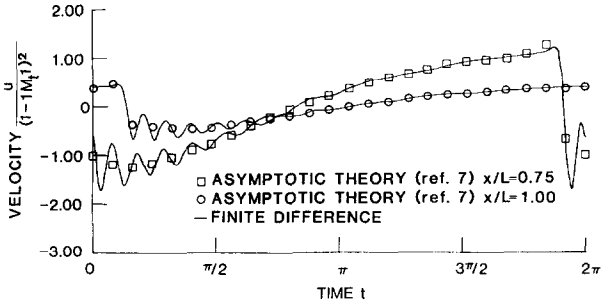

FIG. 7. Acoustic particle velocity without artificial viscosity, 149dB source, $M_t = -0.90$.

ACKNOWLEDGMENTS

The authors would like to acknowledge useful discussions with Drs. A. Bayliss, M. E. Rose, E. Turkel; in particular, hours of discussions with Dr. M. K. Myers.

REFERENCES

1. D. T. BLACKSTOCK, *J. Acoust. Soc. Amer.* **39**, No. 6 (1966), 1019.
2. D. GOTTLIEB AND E. TURKEL, *Math. Comp.* **30** (1976), 703.
3. F. B. GREATRIX, *Trans. Soc. Automot. Eng.* **69** (1961), 312.
4. S. I. HARIHARAN AND H. C. LESTER, *J. Acoust. Soc. Amer.* **75**, No. 4 (1984), 1052.
5. M. G. JONES, "An Experimental Investigation of Sound Attenuation in a High-Subsonic Mach Number Inlet," M. S. thesis, George Washington University, 1982.
6. M. K. MYERS AND A. J. CALLEGHARI, *J. Sound Vib.* **51**, No. 4 (1977), 517.
7. M. K. MYERS, "Shock Development in Sound Transmitted Through a Nearly Chocked Flow," AIAA-81-2012.
8. M. K. MYERS AND A. J. CALLEGHARI, "Acoustic Shocks in Nearly Chocked Flows," AIAA-80-1019.
9. A. H. NAYFEH, J. J. KELLY, AND L. T. WATSON, "Nonlinear Propagation in Near Sonic Flow," AIAA-80-0096.
10. POLYAKOVA, *Soviet Phys. Dokl.* **6**, No. 4 (1961).
11. E. TURKEL, "On the Practical Use of High Order Methods for Hyperbolic Systems," ICASE report No. 78-19, 1978.
12. N. J. WALKINGTON AND W. EVERSMAN, "Finite Difference Solutions to Shocked Acoustic Waves," AIAA-83-0671.